Biogeosciences

Open Access

Bulk partitioning the growing season net ecosystem exchange of CO_2 in Siberian tundra reveals the seasonality of its carbon sequestration strength

B. R. K. Runkle[1], T. Sachs[2], C. Wille[1], E.-M. Pfeiffer[1], and L. Kutzbach[1]

[1]University of Hamburg, KlimaCampus, Institute of Soil Science, Hamburg, Germany
[2]Helmholtz Centre Potsdam – GFZ German Research Centre for Geosciences, Potsdam, Germany

Correspondence to: B. R. K. Runkle (benjamin.runkle@zmaw.de)

Abstract. This paper evaluates the relative contribution of light and temperature on net ecosystem CO_2 uptake during the 2006 growing season in a polygonal tundra ecosystem in the Lena River Delta in Northern Siberia (72°22′ N, 126°30′ E). The occurrence and frequency of warm periods may be an important determinant of the magnitude of the ecosystem's carbon sink function, as they drive temperature-induced changes in respiration. Hot spells during the early portion of the growing season, when the photosynthetic apparatus of vascular plants is not fully developed, are shown to be more influential in creating positive mid-day surface-to-atmosphere net ecosystem CO_2 exchange fluxes than those occurring later in the season. In this work we also develop and present a multi-step bulk flux partition model to better account for tundra plant physiology and the specific light conditions of the arctic region. These conditions preclude the successful use of traditional partition methods that derive a respiration–temperature relationship from all nighttime data or from other bulk approaches that are insensitive to temperature or light stress. Nighttime growing season measurements are rare during the arctic summer, however, so the new method allows for temporal variation in the parameters describing both ecosystem respiration and gross uptake by fitting both processes at the same time. Much of the apparent temperature sensitivity of respiration seen in the traditional partition method is revealed in the new method to reflect seasonal changes in basal respiration rates. Understanding and quantifying the flux partition is an essential precursor to describing links between assimilation and respiration at different timescales, as it allows a more confident evaluation of

measured net exchange over a broader range of environmental conditions. The growing season CO_2 sink estimated by this study is similar to those reported previously for this site, and is substantial enough to withstand the long, low-level respiratory CO_2 release during the rest of the year to maintain the site's CO_2 sink function on an annual basis.

1 Introduction

Amplified arctic warming (Serreze and Francis, 2006; Serreze and Barry, 2011) has created a widespread interest in the CO_2 exchange fluxes of tundra ecosystems (McGuire et al., 2009). There are still a number of unresolved questions regarding the seasonality of key controls on the processes governing this land-atmosphere flux. While all ecosystems respond to the timing and magnitude of hot periods, the short Arctic growing season is particularly sensitive to synoptic weather conditions, including the number and extent of warm weather events characterized by warm, dry winds from the continental south (Johannessen et al., 2004). In this study, we examine how these few, brief warm periods (with air temperatures exceeding 20 °C and approaching peaks near 30 °C for three to five days) have the potential to alter the CO_2 balance of tundra ecosystems.

The net ecosystem exchange (NEE) of CO_2 between the land surface and atmosphere is commonly partitioned between gross primary productivity (P_{gross}) and ecosystem respiration (R_{eco}) as a means to boost understanding of the underlying environmental processes driving these flux terms

(Reichstein et al., 2005) as well as to fill measurement gaps in flux time series (Falge et al., 2001). In the simplest of such methods, the R_{eco} term is often modelled as a function of temperature from nighttime conditions where P_{gross} is assumed to be negligible (Falge et al., 2002), where the choice of air, soil, or surface temperature is made based on the correlation of each with nighttime NEE (Lasslop et al., 2012). This method has been widely applied at arctic sites, despite the seasonal near-absence of truly dark conditions (e.g. Groendahl et al., 2007; Kutzbach et al., 2007; Zamolodchikov et al., 2003), relying on late spring and early autumn nighttime measurements to generate a temperature-R_{eco} relationship for the growing season. Another study using an 11 yr NEE dataset from an eastern Greenland site with a 3.5-month polar day was gap-filled by determining R_{eco} as a residual from a moving-window light response curve, and no temperature relationship was assigned to it (Lund et al., 2012). Other researchers have developed bulk methods which either simultaneously or in stepwise fashion fit the respiratory and uptake contributions together. In the stepwise approach often one or more of the respiration parameters is determined from a best-fit relationship during a moving window or seasonal model, and the other parameters are then found with this fixed parameter held constant (Lasslop et al., 2010; Parmentier et al., 2011). These approaches often require setting a radiation-based threshold to separate day and nighttime periods (e.g. 20 W m^{-2} in the adaptation of Lasslop et al., 2010, in the polar Siberian work of Parmentier et al., 2011).

In order to more fully elucidate the seasonality of flux-governing parameters, this paper tests a time-sensitive approach where the NEE time series is analyzed in one-week increments as the combination of a temperature-dependent R_{eco} flux and a PAR-dependent flux (i.e. P_{gross}). While this method assigns much of the temperature-correlated NEE flux to R_{eco}, it still allows for detection of temperature-based influences on the P_{gross} flux through examining the correlation of the residuals of a light response model to temperature. Both flux components are known to be temperature-sensitive. The general temperature response of ecosystem respiration is well defined (Mahecha et al., 2010; Yvon-Durocher et al., 2012), including descriptions of increases in decomposition with temperature for sedge litter (Thormann et al., 2004). Extensive research has also demonstrated the temperature dependence of the photosynthetic apparatus (e.g. Berry and Björkman, 1980; Medlyn et al., 2002). Particularly in some moss-sedge environments, high-temperature stress on photosynthetic performance has been quantified in studies at the closed chamber level (i.e. 60×60 cm squares) (Riutta et al., 2007) and in leaf- or shoot-level measurements (Williams and Flanagan, 1998). As such, these effects are often incorporated into soil-vegetation-atmosphere transfer models that upscale arctic leaf-scale fluxes to the footprint of an eddy covariance tower and to larger scales (Williams and Rastetter, 1999), though not always (Shaver et al., 2007). However, photosynthetic deactivation driven by higher temperature is

often not considered important on seasonal timescales due to tundra mosses' relatively high optimal temperatures and ability to adapt quickly (Furness and Grime, 1982; Oechel, 1976; Riutta et al., 2007; Sveinbjörnsson and Oechel, 1983; Zona et al., 2011). Similarly, the tussock tundra species *Eriophorum vaginatum* has been found to have only a minimal physiological response to temperature (Tissue and Oechel, 1987).

Photosynthesis is a light-sensitive process governed at first order on the ecosystem level by incoming light levels (Haxeltine and Prentice, 1996). Plants can also adapt over timescales of days to changes in photoperiod and other light conditions (Bauerle et al., 2012). On the other hand, certain *Sphagnum* moss species face photoinhibition or light stress (Murray et al., 1993), in part as a response to low tissue nitrogen levels weakening photosystem II's adaptive capacity (Henley et al., 1991; Long et al., 1994). This reaction was explored in a laboratory study exposing mosses to light treatments with photosynthetically active radiation (PAR) set to 800, 340, and 150 µmol m^{-2} s^{-1}; only the treatment at 800 µmol m^{-2} s^{-1} faced signs of light-induced inhibition of photosynthesis (Murray et al., 1993). Light stress in tundra moss species has also been shown to be greater early in the season, with subsurface morphological adaptations to this stress sustaining more late-season photosynthesis and delayed senescence (Zona et al., 2011). Similar morphological adaptations have been seen in open bog boreal *Sphagnum* species (Hájek et al., 2009). A partition method should then be receptive to the possibility of light and temperature sensitivities that change through the season. These stresses (or process amplifiers) may be apparent through an examination of the daytime residuals of a light-response model.

The specific objectives of this study are to:

1. Test the proposed bulk flux-partition method against more traditional procedures for a low arctic tundra ecosystem.

2. Determine the growing season NEE flux and temporal changes in the relative strength of its two partitioned components R_{eco} and P_{gross}.

3. Analyze the short-term net CO_2 flux during hot spells in a tundra ecosystem.

4. Examine the effect of the timing of hot periods in the ecosystem's growing season carbon balance.

2   Site description

The study site is located on Samoylov Island (5 km^2), 120 km south of the Arctic Ocean in the southern central Lena River Delta (72°22′ N, 126°30′ E), and is considered representative of the region's modern delta areas that include a late Holocene river terrace and different active floodplain levels, and cover about 65 % of the total delta area. Over the past fourteen years, a variety of investigations has been performed

at the site, including studies on landscape-scale gas and energy exchange, soil science, hydrobiology, microbiology, and geomorphology (Hubberten et al., 2006; Boike et al., 2012). The study site is located in the central part of the island's 3 km^2 late Holocene river terrace and contains mostly flat macrorelief with elevations from 10 to 16 m a.s.l. The surface of the terrace features wet polygonal tundra, whose development has created regular microrelief with typical elevation differences of around 0.5 m between depressed polygon centers and elevated polygon rims (Kutzbach, 2006). These landscape units contain a large pool of accumulated organic matter – greater than 25 kg m^{-2} soil organic carbon in the top 1 m (Zubrzycki et al., 2012) – facing slow decomposition rates due to low annual temperatures and chemical recalcitrance (Höfle et al., 2012).

The site has a true arctic continental climate with very low temperatures and low precipitation. Mean annual conditions at the site's meteorological station have been determined from 1999 to 2005, and include mean air temperature of −14.7°C and mean summer precipitation of 137 mm, ranging from 72 mm to 208 mm in this period (Boike et al., 2008). Frequent cyclonic activity in the area causes rapidly changing weather conditions throughout the growing season by advection of cold and moist air from the Arctic Ocean or warm and dry air from continental Siberia, respectively. Polar day lasts from 7 May to 8 August, and polar night lasts from 15 November to 28 January. Typically, snowmelt and river break up start in the first half of June, and the growing season lasts from mid-June through mid-September. The delta's continuous permafrost reaches depths of 500 to 600 m (Grigoriev, 1960) and is characterized by relatively low temperatures with the top-of-permafrost (1.7 m) temperature on Samoylov measured as approximately −7.8°C from 2006 to 2011 (Boike et al., 2003, 2012).

The wet polygon centers and their edges are dominated by hydrophytic sedges such as *Carex aquatilis*, *Carex chordorrhiza*, and *Carex rariflora* as well as moss species that include *Drepanocladus revolvens*, *Meesia triquetra*, and *Aulacomnium turgidum* (Kutzbach et al., 2004; Sachs et al., 2008). Plant cover on the polygon rims is dominated by mesophytic dwarf shrubs such as *Dryas octopetala* and *Salix glauca*, forbs (*Astragalus frigidus*), and mosses (*Hylocomium splendens*, *Timmia austriaca*). Mosses and vascular plants are estimated to cover 95 % and 30 %, respectively, of both the depressed centers and their surrounding rims (Kutzbach et al., 2004). Surface classification of high-resolution aerial photographs taken in the eddy footprint region of the island in 2003 shows that elevated and dryer polygon rims cover approximately 60 % of the area surrounding the study site, while depressed and wet polygon centers and troughs cover 40 % of the area (G. Grosse, personal communication, 2005). The onset of greening in the study year (2006) occurred around 10 June, which is the earliest date when the 8-day MODIS LAI product is non-zero (i.e. 0.1 m^2 m^{-2}, relative to season high 0.5 m^2 m^{-2} on

12 July) (ORNL DAAC, 2013). Leaf senescence in the study year (2006) occurred in the period between 26 August and 9 September.

3 Methods

3.1 Eddy covariance and meteorological data collection

An eddy covariance system with a closed-path CO_2 and H_2O gas analyzer (LI-7000, LI-COR Biosciences, USA) measured the turbulent fluxes of momentum, heat, CO_2 and H_2O from 9 June to 19 September 2006. An ultrasonic anemometer (Solent R3, Gill Instruments Ltd, UK) measured wind velocity components in three dimensions and sonic temperature at 20 Hz frequency from a height of 4 m. Sample air was drawn at a rate of 20 L min^{-1} from the air intake 15 cm below the anemometer measurement point, through a polyethylene/aluminium composite wall tube of 5-m length and 6.375-mm inner diameter (Dekabon$^®$ 1300) to the closed path gas analyzer. All analog signals were synchronously digitized at 20 Hz and logged on a laptop PC running EdiSol software (J. Massheder, University of Edinburgh, UK). The system was powered by a diesel generator located 100 m southwest from the tower in the least frequent wind direction, and an auxiliary, uninterruptible AC power supply device provided continuous operation.

This site was supported by an adjacent meteorological station that collected data on relative humidity and air temperature (MP103A, ROTRONIC AG, Switzerland), air pressure (RPT410F, Druck Messtechnik GmbH, Germany), photosynthetically active radiation (PAR; QS2, Delta-T Devices Ltd., UK) and the incoming and reflected components of short-wave and longwave radiation, respectively (CNR 1, Kipp and Zonen, Netherlands). Surface temperature (T_s) was determined from the outgoing longwave radiation measurement with the Stefan–Boltzmann law and an assumed emissivity of 0.98. Precipitation and soil temperature data were recorded at a long-term monitoring station 700 m south of the eddy covariance tower (Boike et al., 2008). The site's fetch is relatively flat and homogeneous despite the microtopographic variation in the polygonal surface (Kutzbach et al., 2007; Sachs et al., 2008; Wille et al., 2008).

Our flux-data processing and correction routine is presented and summarized in Table 1, and included data screens based on stationarity, instrument performance, and integral turbulence characteristics (Foken and Wichura, 1996). Flux data are presented using the atmospheric convention, where positive values represent a net upward flux, and negative values represent net downward fluxes (i.e. where photosynthetic uptake is dominant).

3.2 Data analysis and flux partitioning

Several partition models are used to separate the net CO_2 flux (NEE) into gross primary productivity (the

Table 1. Flux data processing routine, implemented in EdiRe (R. Clement, University of Edinburgh, UK).

Despike the three wind vector and sonic temperature time series using a detection method based on deviations further than a set number of standard deviations from a moving window mean (Vickers and Mahrt, 1997). The T_s- and w-series were despiked using a 4.5 standard deviation threshold, the u-, v-, and CO_2-series were despiked using a 4.0 standard deviation threshold, and the H_2O-series was despiked using a 3.5 standard deviation threshold, reflecting their different probability distributions.

Angle of attack correction for the response of the sonic anemometer (Nakai et al., 2006).

Double coordinate rotation in order to: (i) rotate u into the mean horizontal wind and (ii) reduce mean w to zero.

Linearly de-trend the scalar time series and calculation of flux estimate.

Determine cross-correlation sequence of 30-min interval to find the lag time which maximizes the covariance of scalar transport (i.e. $\overline{w's'}$, the covariance of the fluctuations of the molar concentration of scalar s' and the vertical wind fluctuations w') and de-lag the time series of s.

Webb-Pearman-Leuning terms (WPL) are applied to the CO_2 signal (Leuning, 2007; Webb et al., 1980) with a latent heat flux (LE) determined using the lag time to maximum covariance of CO_2, rather than H_2O (Ibrom et al., 2007), i.e. LE_{WPL}.

Apply frequency response corrections (Moore, 1986) for each sensor:
    sonic path length,
    sensor separation between the sonic and gas sampling,
    tube attenuation,
    signal high-pass filtering (linear de-trend),
    temporal averaging due to the sample lifetime in the cell,
    spatial averaging at the sample intake.

The CO_2 signal is additionally corrected with a first-order low-pass filter with time constant 0.3183 s for the period prior to 20 June 2006, when the LI-7000 low pass filter was set to 1 s.

Correction of sensible heat flux (Schotanus et al., 1983) and calculation of Obhukov stability parameter.

Evaluate integral turbulence characteristics and stationarity (Foken and Wichura, 1996) in 30-min period for use in filtering out inadequate flux measurements.

Removal of data in a 30° mean wind-direction window (238–268°) due to contaminating influence by the diesel generator used to power eddy-covariance equipment (Sachs et al., 2008).

---

atmosphere-surface flux, P_{gross}) and ecosystem respiration (the surface-atmosphere flux, R_{eco}). In general, the PAR-sensitive portion of measured NEE is assigned to P_{gross} and at least part of the temperature-sensitive portion of NEE is assigned to R_{eco}. The NEE fluxes are first partitioned in a "traditional model" (as in Kutzbach et al., 2007) by assuming that fluxes during low-light periods (PAR < 20 μmol m^{-2} s^{-1}) are fully composed of ecosystem respiration, are an exponential function of surface temperature, and are not a function of PAR. These flux measurements are pooled for a single best-fit relationship between R_{eco} and T_s, using the empirical Q_{10} model (van't Hoff, 1898)

$$R_{eco,1} = R_{base,1} Q_{10,1}^{\frac{T_{s,-T_{ref}}}{\gamma}}, \tag{1}$$

where, as in Mahecha et al. (2010), $T_{ref} = 15°C$ and $\gamma = 10°C$ are independent parameters held constant, $Q_{10,1}$ is a best-fit parameter indicating sensitivity of ecosystem respiration to surface temperature, and $R_{base,1}$ is a best-fit parameter indicating basal respiration at the reference temperature T_{ref}. $R_{eco,1}$ is the modelled respiration flux. The Q_{10} model is comparable to the exponential relationship

$R_{eco,exp} = R_b \exp(k_{T,1} T_s)$, where $k_{T,1}$ and R_b are best fit parameters, used in Kutzbach et al. (2007). Surface temperature is used as the regressor variable here, based on favourable comparisons to air temperature and based on previous experience at this site (Kutzbach et al., 2007), though air temperature is also commonly used to model tundra ecosystem respiration (Loranty et al., 2010; Rastetter et al., 2009).

The P_{gross} portion of the flux is then estimated from the difference between measured NEE and modelled $R_{eco,1}$, and is modelled as a function of PAR, using the rectangular hyperbola function

$$P_{gross,1} = -\frac{P_{max,1}\alpha_1 PAR}{P_{max,1} + \alpha_1 PAR}. \tag{2}$$

The fit parameters α_1 and $P_{max,1}$ represent, respectively, the initial canopy quantum efficiency (that is, the initial slope of the P_{gross}-PAR curve at PAR = 0) and the maximum canopy photosynthetic potential, which is the hypothetical maximum of P_{gross} at infinite PAR; $P_{gross,1}$ is the modelled CO_2 uptake using this approach. Both α_1 and $P_{max,1}$ are assumed to have positive values, necessitating the negative sign on the

equation's right-hand side to allow P_{gross} to fit the NEE sign convention. This model contains the explicit assumption that the gross productivity flux is not influenced by light stress or temperature effects. This model is parameterized for each 7-day interval during the measurement period.

A different two-step "bulk model" proposed here is developed to allow its governing parameters to change over the measurement period and to enable a portion of the low-light flux to be assigned to P_{gross}. This method first fits both a parabolic light curve and a temperature response to the NEE flux measured when PAR $< 500\,\mu\text{mol}\,\text{m}^{-2}\,\text{s}^{-1}$, thus below the range where light stress on P_{gross} is expected to occur (Murray et al., 1993) yet high enough to include enough data to parameterize the light-response hyperbola. The model is a best fit of the parameters α_2, $P_{\text{max},2}$, $R_{\text{base},2}$, and $Q_{10,2}$, for 7-day intervals during the measurement period using the following function:

$$F_{\text{CO}_2} = \text{NEE} = P_{\text{gross},2} + R_{\text{eco},2} = -\frac{P_{\text{max},2}\alpha_2 \text{PAR}}{P_{\text{max},2} + \alpha_2 \text{PAR}}$$
$$+ R_{\text{base},2} Q_{10,2}^{\frac{T_s - T_{\text{ref}}}{\gamma}} . \quad (3)$$

The NEE time series is then partitioned in 7-day intervals using $R_{\text{base},2}$ and $Q_{10,2}$ to estimate $R_{\text{eco},2}$ and setting the residual flux to $P_{\text{gross},2}$. This derived P_{gross} flux term is then modelled by refitting a light-response curve across the whole range of incoming PAR using a new pair of positive-valued parameters, α_3 and $P_{\text{max},3}$:

$$P_{\text{gross},2} = \text{NEE} - R_{\text{base},2} Q_{10,2}^{\frac{T_s - T_{\text{ref}}}{\gamma}} = -\frac{P_{\text{max},3}\alpha_3 \text{PAR}}{P_{\text{max},3} + \alpha_3 \text{PAR}}. \quad (4)$$

Parameters in both sets of models are found via unconstrained nonlinear regression to minimize the mean-square-error of the residuals (i.e. the *nlinfit* function in Matlab Release R2011b, The Mathworks, Inc.). The parameter 95% confidence intervals are determined using the Jacobian matrix computed in the nonlinear fitting (i.e. using Matlab's *nlparci* function); these are used to generate an error propagation estimate on modelled fluxes. This error propagation method assumes a normally distributed random relative error of 20% on measured NEE fluxes, which is on the conservative end of the range estimated in previous works (Wesely and Hart, 1985; Moncrieff et al., 1996), so is analogous to the 95% confidence intervals used on the parameters. For the gap-filled points in the time series we use the model parameter 95% uncertainty estimates in a first-order partial derivative of the respective model equations (i.e. Eqs. 2–4). The final error estimate for the cumulative fluxes is then defined according to the following equation, relating individual flux errors to the cumulative value in quadrature:

$$u_{F_{\text{cumul}}} = \sqrt{d_{\text{int}}^2 \sum_{i=0}^{n} u_{F-i}^2} = d_{\text{int}}\sqrt{\sum_{i=0}^{n} u_{F-i}^2}, \quad (5)$$

where $u_{F_{\text{cumul}}}$ is the cumulative flux uncertainty, d_{int} is the interval length (i.e. 30 min), n is the number of intervals, and u_{F-i}^2 is the estimated uncertainty for each (i-th) 30-min flux (either measured or modelled).

The choice of modelling with 7-day intervals rather than a moving window rests in the desire to identify periods with temperature or light stress. Including more than the 3–5 days used in other studies is necessary in order to include enough data from both similar phenological conditions and different meteorological conditions. For example, a sufficient temperature range is needed for an appropriate estimation of the respiration temperature sensitivity parameter $Q_{10,2}$, i.e. the curvature of the respiration-temperature relation. Given some scatter in the data, a narrow temperature range could cause errors in estimating this term, with consequences for the $R_{b,3}$ term as well. The moving window approach may be more useful for gap-filling but the fixed interval approach is valuable for gathering quasi-independent time slices of data from which to examine light and temperature responses.

3.3 Sensitivity to the timing of warm spells

The sensitivity of the ecosystem's mid-day sink-source function to warm spell timing is investigated using the two partition models to determine the threshold temperature ($T_{s,\text{TH}}$) at which mid-day CO_2 flux turns positive (i.e. from surface to atmosphere). This modelling is performed using the daily maximum PAR value (PAR_{max}) measured for each day of the measurement period. The modelled $T_{s,\text{TH}}$ is therefore an inversion of the full NEE model (i.e. Eq. 4 for the bulk case), where NEE is set to 0 and the PAR term is set to PAR_{max}:

$$T_{s,\text{TH}} = \frac{\gamma}{\ln\left(Q_{10,2}\right)} \ln\left[\frac{P_{\text{max},3}\alpha_3 \text{PAR}_{\text{max}}}{P_{\text{max},3} + \alpha_3 \text{PAR}_{\text{max}}} \frac{1}{R_{\text{base},2}}\right] + T_{\text{ref}}. \quad (6)$$

4 Results

Meteorological conditions during the 2006 growing season (Fig. 1) were characterized by air temperatures between 0 and 29 °C, high humidity, and strong diurnal fluctuations in light. This period included two locally extreme warm periods ($T_{\text{air}} > 25$°C) around days of year (DOY) 192 and 212, which also included vapour pressure deficits (VPD) greater than 1.5 kPa. There were approximately four other identifiable warm periods (around days of year 166, 203–207, 230, and 237). Relative humidity fell below 50% only during the hot periods on days 166, 192, and 212; periods during days 166, 212, and 237 were characterized by winds from the south. Air temperature remained continuously above the freezing point from 25 June to 1 September. During the bulk of the growing season, the maximum light received (i.e. as PAR), declined on a day-to-day basis, with several intermittent week-long cloudy periods. Daily NEE fluxes were consistently negative between 28 June (DOY 179) and 2 August
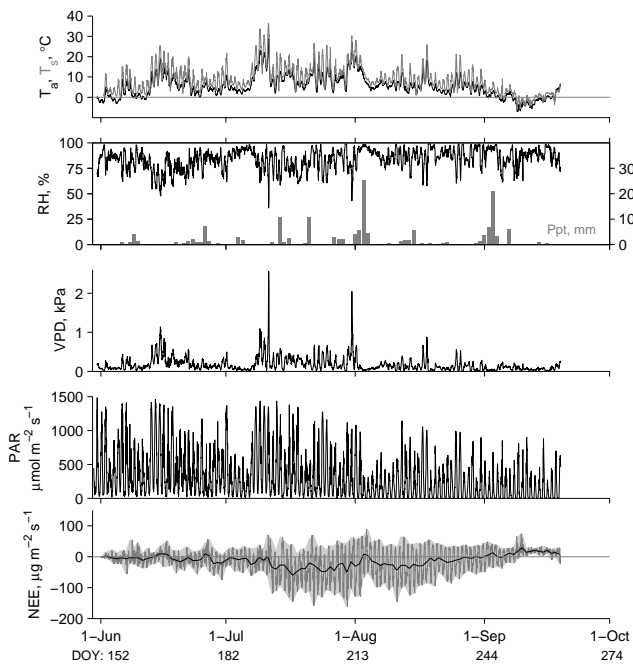
Fig. 1. Meteorological conditions and gap-filled eddy covariance measurements of the CO_2 flux for the growing season measurement period, 2006; Samoylov Island site, Lena River Delta, Russia. The meteorological data shown are air temperature (T_a), surface temperature (T_s) derived from outgoing longwave radiation, relative humidity (RH), vapour pressure deficit (VPD), and photosynthetically active radiation (PAR). The bottom panel presents the daily mean CO_2 flux measurements in a darker line, half-hourly estimates of net ecosystem exchange of CO_2 (NEE) in gray, and the daily range in light gray. The time series is given in calendar dates as well as day of year (DOY).

(DOY 214), and following a two-day net CO_2 release were again negative until 30 August (DOY 242). Cumulative NEE included a large sustained uptake from 12 July (DOY 193) to 2 August (DOY 214) (also shown in Fig. 6). The two-day net CO_2 release in early August coincided with a major storm event with more than 35 mm rainfall, daily maximum PAR levels below $500\,\mu\mathrm{mol\,m^{-2}\,s^{-1}}$, and wind speeds regularly exceeding $8\,\mathrm{m\,s^{-1}}$.

The partition models generated different parameterizations for the CO_2 fluxes (Fig. 2). The exponential relationship of $R_{\mathrm{eco},1}$ to surface temperature used in the traditional partition model had parameters $R_{\mathrm{base},1} = 56.4 \pm 3.1\,\mu\mathrm{g\,m^{-2}\,s^{-1}}$ and $Q_{10,1} = 1.88 \pm 0.12$ in a model that yields $r^2 = 0.43$ and root mean square error (rmse) $= 8.6\,\mu\mathrm{g\,m^{-2}\,s^{-1}}$, with $n = 448$ measurement intervals contributing to this model. This model of $R_{\mathrm{eco},1}$ with surface temperature explained low-light NEE fluxes better than a trial model fit to air temperature ($r^2 = 0.37$; rmse $= 9.0\,\mu\mathrm{g\,m^{-2}\,s^{-1}}$). When compared to the traditional method (Fig. 2), the weekly fitted parameters of the new bulk partition method tended to have a lower temperature response ($Q_{10,2} = 1.52 \pm 0.33$) and more variation in

the basal respiration rate ($R_{\mathrm{base},2} = 54.1 \pm 13.3\,\mu\mathrm{g\,m^{-2}\,s^{-1}}$). Additionally, the weekly $P_{\mathrm{max},1}$ estimates of the traditional method tended to be higher than those of the bulk method, while the light response parameter α tended to be higher in the bulk method. Best-fit values of α_3 in the bulk method vary between 0.16 and 0.95 µg (CO_2) $\mu\mathrm{mol}^{-1}$ (quanta), compared to a range of 0.26 to 0.75 $\mu\mathrm{g\,\mu mol^{-1}}$ in the traditional model for α_1. The bulk model slightly reduced the r.m.s.e. relative to the traditional model (on average, by 5 % each week). The traditional partitioning model, relative to the bulk model, created residuals that are more often correlated to temperature (9 vs. 2 7-day intervals, respectively) (Fig. 2c). In these cases, both of the models significantly overpredicted CO_2 fluxes at higher temperatures (i.e. the NEE magnitude was higher, and the models predicted greater respiratory or lower uptake fluxes).
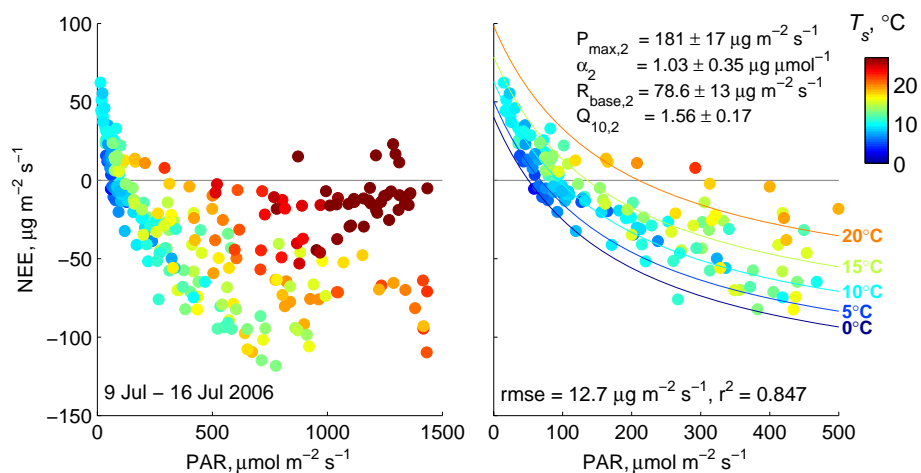
The bulk partitioning model (i.e. Eq. 3) has been fit to 7-day time slices of NEE, PAR and T_s measurements. One example of this fit for the period containing the first of the hot spells (9–16 July) demonstrates how such a hot period may induce positive CO_2 fluxes during mid-day high-PAR conditions theoretically optimal for photosynthetic CO_2 uptake (Fig. 3). Applying the new bulk partition method revealed relatively high basal respiration rates with moderate temperature dependence. This period preceded the ecosystem's maximum light response so that even with this moderate temperature sensitivity, the higher respiratory fluxes outpaced any responses in uptake to higher light or temperature. The data from this period, shown in Fig. 3, also highlight the strong response to increases in both light and temperature even in the lowest light region. This response is evident from the relatively high light use efficiency ($\alpha_2 = 1.03 \pm 0.35\,\mu\mathrm{g\,\mu mol^{-1}}$) that reduced net fluxes at low light.

The resultant partitioned fluxes from the bulk method are shown in Fig. 4. This partition highlights several environmental processes. First, there was a slow ramping up of $P_{\mathrm{max},3}$, which peaked at $240 \pm 11\,\mu\mathrm{g\,m^{-2}\,s^{-1}}$ during the first week in August (this process is also evident in Fig. 2e; the traditional partition method estimated $334 \pm 23\,\mu\mathrm{g\,m^{-2}\,s^{-1}}$ for $P_{\mathrm{max},1}$ during this period) and remained rather high with a steady decline following the pattern of vegetation senescence until freezing a month later. Second, there was little evidence of either light stress or a temperature response within the light curve (this finding is also demonstrated statistically through the residuals analysis in Fig. 2c). Third, due to the synchronicity of surface temperature and light in the diurnal cycle, the respiratory fluxes tended to peak at the highest light levels.

The ecosystem's positive mid-day NEE in response to higher temperatures (as highlighted in Fig. 3) is explored in more detail by finding the threshold temperature at which the NEE turns positive for the PAR time series of this growing season (Fig. 5). A model was derived from each partition method to show when the ecosystem was susceptible to this mid-day efflux of CO_2. The mid-season increase in
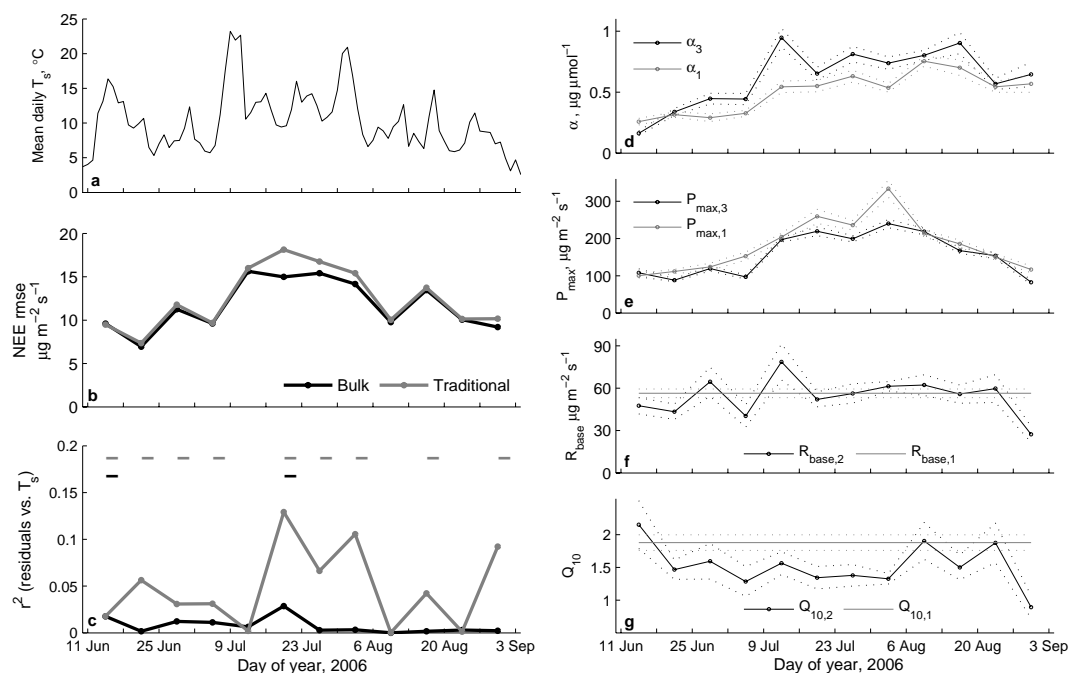
Fig. 2. (a) A time series of mean daily surface temperature is shown for comparative purposes. Time series of fitting statistics include **(b)** root mean square error (rmse) between the NEE data and models and **(c)** coefficient of determination (r^2) between NEE model residuals and surface temperature (T_s). The sign of this correlation (when significant, with $p < 0.05$) is given above each time interval. For example, residuals of the traditional model (in grey) are negatively correlated to temperature between 11 June and 9 July 2006; in these time periods the model would overpredict CO_2 fluxes at higher temperatures. Time series of NEE parameters from the new, weekly fit bulk method (in black) and the traditional method (in grey) through the measurement period are presented with parameter confidence intervals shown in dotted lines. These parameters are the initial quantum efficiency α **(d)**, maximum canopy photosynthetic potential P_{max} **(e)**, basal respiration R_{base} **(f)**, and respiration sensitivity term Q_{10} **(g)**.


Fig. 3. NEE flux measurements during period 9 July–16 July, 2006 (i.e. days 190–197), plotted against PAR and coloured according to surface temperature. The right-hand panel provides an example of the bulk flux partition model (i.e. Eq. 3) in the low PAR range during this period with five of the fitted isotherms provided for comparison. Note the change in the plotting range of the x-axis between the two images.

photosynthetic capacity (determined through the P_{max} parameters) increased the threshold temperature so much as to make this response very unlikely. Later season heat spells were less likely to generate a net positive CO_2 flux, whereas

earlier heat spells were able to generate this mid-day positive NEE flux (i.e. occurring when the surface temperature exceeded the threshold temperature). The moss community together with what vascular plant activity existed at this time
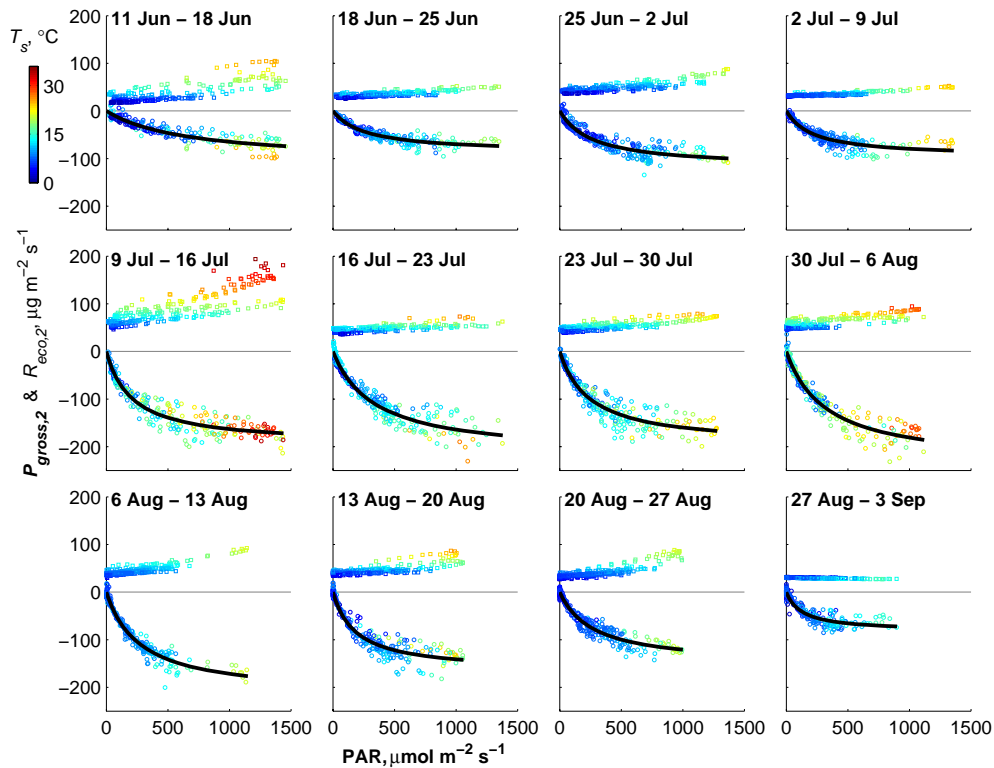
Fig. 4. Time series of scatter plots showing the NEE flux partitioned into modelled photosynthesis $P_{\mathrm{gross},2}$ and modelled ecosystem respiration $R_{\mathrm{eco},2}$, plotted against PAR, with points colored according to surface temperature (T_{s}) and generated according to the bulk method described in the text (i.e. Eqs. 3–4). The $P_{\mathrm{gross},2}$ model's light-response parameters ($P_{\mathrm{max},3}$, α_3) are fit to each time slice by minimizing the root mean square of the residuals (rmse). $P_{\mathrm{gross},2}$ and $R_{\mathrm{eco},2}$ have units of $\mu\mathrm{g\,m^{-2}\,s^{-1}}$. Each subplot represents a different one-week time period.
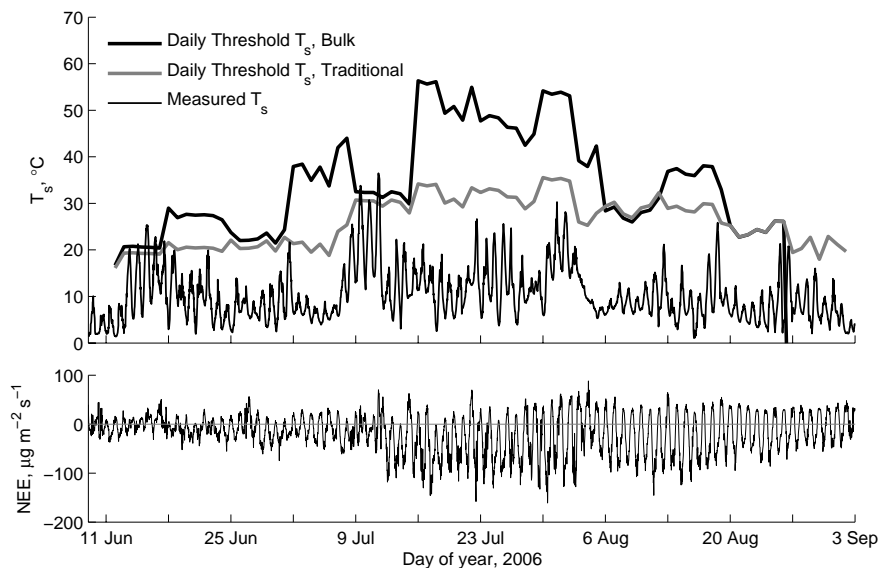
Fig. 5. Ecosystem sensitivity to surface temperature, with respect to positive mid-day CO_2 fluxes generated using measured PAR time series for the 2006 growing season with model parameters generated as described in the text (Eq. 6). Surface temperatures higher than the threshold would enable net positive mid-day CO_2 fluxes. The NEE time series is re-printed from Fig. 1 in the lower panel to ease comparison.

did not take up enough CO_2 to exceed respiration during these periods. The bulk partition method generated higher temperature thresholds than the traditional partition method, reflecting its assignment of some of the low-light NEE flux to uptake rather than to dampen respiratory activity. More generally, the relatively lower threshold periods in this figure (such as following 6 August or 20 August) represent a response to synoptic weather conditions, when cloudier (lower PAR) conditions lower photosynthetic uptake and so required less respiration to offset P_{gross}. The mid-day net CO_2 release events driven by early season high temperatures differ from cumulative net CO_2 releases in the period 3–5 August. During this period low radiation, high precipitation, and high wind speeds dampened photosynthesis enough to create net positive fluxes (seen in Fig. 1).

The net outcome of this work is an NEE flux time series that is gap-filled and partitioned using the two methods; these cumulative seasonal fluxes are shown in Fig. 6. Both methods suggested an unambiguous sink function, with partitioned fluxes changing relatively little ($< 10\%$) between methods at this timescale. Using the traditional partition method for gap-filling yielded a greater sink function (a larger magnitude of NEE) by partitioning less of the NEE flux to respiration than in the bulk partition case. All three fluxes showed an inflection near day 190 (i.e. 9 July), after which the fluxes (in particular, the P_{gross} flux) increased substantially until day 215 (i.e. 3 August), when the rate of increase slowed. The ecosystem's carbon sink function was nearly finished at day 240 (i.e. 28 August), when the upward and downward flux terms were in balance. Partitioning after day 246 (i.e. 3 September) was discarded due to the sustained positive fluxes in this period and negative correlation with temperature. This period behaved differently, ecologically, due to its freezing temperatures, onset of snowfall, and late August leaf senescence.

5 Discussion

There are challenges in partitioning NEE into R_{eco} and P_{gross} during the long polar day; in particular, separating temperature effects between the two flux portions may involve an extrapolation out of the conditions used for parameterization. Understanding the net effect of these environmental flux drivers is important in determining present-day carbon balances and cycling as well as making predictive models for these landscapes. In this paper, the multi-step partition method used to model NEE fluxes implicitly assumes that all of the temperature sensitivity of NEE in the low PAR range is revealed through changes in the R_{eco} parameters, and are therefore unrelated to changes in the P_{gross} portion of the net flux. This decision appears justified by the general lack of correlation between the bulk model's residuals and temperature, even when the full PAR range is considered.

There are a number of benefits of the multi-step bulk partitioning method considered here. First, the method allows
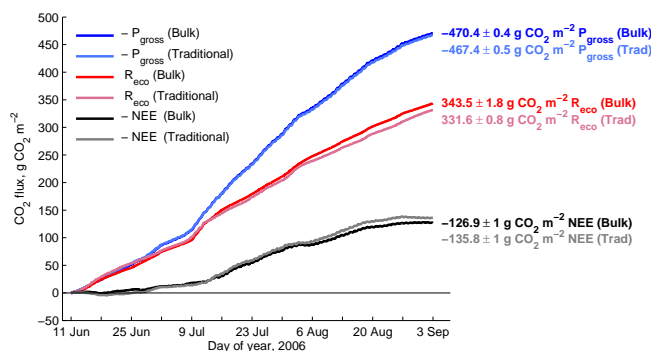
Fig. 6. Cumulative, gap-filled CO_2 fluxes for an 84 day period (11 June–3 September 2006) using different models, where the bulk model is the multi-step approach developed in this paper and the traditional model is also described in the text. Note the sign-switching for P_{gross} and NEE to ease comparison with R_{eco}. Gap-filling was necessary for 21 % of the 4032 measurement intervals considered in this period, and creates the differences between the two methods' cumulative NEE fluxes. Error propagation assumes 20 % randomly distributed relative error as 95 % confidence intervals on the flux measurements and the derived 95 % confidence intervals on the flux partition parameters; these are combined in quadrature (Eq. 5).

one to discover the seasonality of the respiration parameters during a season where very few measurement points support the traditional parameterization scheme. In particular, the basal respiration parameter increased during mid-season when using the newer method, and the temperature sensitivity parameter (Q_{10}) decreased (from 1.9 to mean 1.5). This shift implies that the traditional method would overestimate respiratory responses to temperature, whereas actually the base respiration had a stronger phenological pattern. This phenology may follow from seasonal growth in the overall microbial biomass, increases in the thaw depth that allow a greater contributing soil volume to total respiration fluxes, and larger mid-summer contributions from plant respiration to R_{eco}. Such a change in interpreting the R_{eco} flux follows recent work demonstrating that temperature sensitivity is often overestimated at the expense of ignoring seasonal changes in base respiration (Mahecha et al., 2010).

A second benefit to the bulk partition method is its use of a broader range of environmental conditions to parameterize the respiration flux, thus reducing the range of temperatures into which the respiration model needs to extrapolate. For example, while the maximum surface temperature found in this study was 36.5 °C, the maximum temperature during PAR conditions less than 500 μmol m^{-2} s^{-1} (the bulk method's threshold for the initial combined R_{eco}-P_{gross} parameterization) was 26.2 °C, and the maximum temperature under PAR conditions less than 20 μmol m^{-2} s^{-1} (the traditional threshold for nighttime conditions) was 17.6 °C. Thus a portion of the uncertainty in extending nighttime temperature relationships during the much warmer daytime has been removed in this model. Yet, the new method still may allow

for the discovery of ecosystem-wide deactivation in response to higher light and/or higher temperature (both of which, in this case, seem minimal). Finally, the new method also avoids extrapolation of R_{eco} under dark conditions to R_{eco} under light conditions, when leaf respiration may be inhibited by up to 20 % (Brooks and Farquhar, 1985; Wohlfahrt et al., 2005).

Limits remain for both partitioning model strategies. The methods are only parameterized under existing environmental conditions, so they are unable to help in suggesting how the ecosystem may acclimate to changes in the timing, magnitude, or duration of hot periods. Additionally, the drying of the land surface (i.e. reduced soil moisture or changes in water table) or of the air (in terms of humidity) are not considered. However, the relatively few low humidity periods (VPD > 1 kPa) prevent a proper parameterization of a model representing these effects. Moreover, their scarcity may prevent the need (or ability) for such a model in this landscape, though there may be some risk that not including these effects artificially inflates the temperature effect on the respiration portion of NEE (Lasslop et al., 2010). An additional challenge is that neither method accounts for variation in the contributions to P_{gross}, e.g., mosses and vascular plants are governed by different light-response mechanisms and parameters – nor to R_{eco}, e.g., differences across the microtopographic zones (dryer polygon rims, inundated centers). Encouraging progress has been made elsewhere on parts of this question (Belshe et al., 2012) though a full footprint contribution model would be overparameterized for the time series presented here.

The NEE estimate for the growing season presented here $(-126.9 \pm 1\,\mathrm{g\,m^{-2}})$ is similar to one presented previously for this site (for a synthetic year combining the end of 2003 and start of 2004 growing seasons), which presented NEE of $-119\,\mathrm{g\,m^{-2}}$ during June–August (Kutzbach et al., 2007). In that work, the authors estimated a moderate CO_2 source for the rest of the year by interpolating between beginning-of-winter and end-of-winter measurements $(+48\,\mathrm{g\,m^{-2}})$, implying that in both cases, the site is a CO_2 sink even on an annual basis. In the season presented here, previous work has demonstrated an ecosystem CH_4 source function of $1.93\,\mathrm{g\,CH_4\,m^{-2}}$ (equivalent in C terms to $5.3\,\mathrm{g\,CO_2\,m^{-2}}$), using both eddy covariance and closed chamber methods (Sachs et al., 2008, 2010). Thus the vertical CO_2 flux sink strength is substantially greater than CH_4 emissions. It is also stronger than the CO_2 source-strength of respiration, which includes outgassing from flooded area and ponds (Abnizova et al., 2012) that cover up to 28 % of the eddy footprint, and which appear to be adequately parameterized within the respiration model used here. Lateral releases of dissolved organic and inorganic carbon are also expected to be much less than the net CO_2 sink, due to the site's flat landscape, pronounced microrelief, ponding and low thaw depth. These factors together prevent lateral water fluxes from the polygon centers through most of the growing season, also keeping catchment-scale export fluxes low (Helbig et al., 2013).

In addition to the season-wide results, this study has also demonstrated how early-season hot periods, prior to full leaf development, generate positive net CO_2 emissions despite high light levels. Additionally, in the tundra region, cool temperatures from the just-thawing active soil layer may also inhibit plant growth during this period. The hot periods may, however, hasten the onset of sedge greening or bud burst, which at least in several tundra shrub species has been shown to have a strong dependence on cumulative heat-based forcing units (i.e. the time-integrated temperature relative to a threshold value commonly set to 0 °C) (Pop et al., 2000). An earlier or longer growing season, however, may not contribute to greater net carbon uptake in these environments due to the rise in R_{eco} caused by warmer temperatures (Parmentier et al., 2011). In the future, a sensitivity analysis of the timing, magnitude, and duration of these events could be performed to show the importance of synoptic meteorological conditions on temporal changes to the local carbon budget. This question is especially urgent given likely consequences of changes in Arctic sea ice coverage and the resultant modifications of the balance between continentally and Arctic Ocean-derived weather systems (Deser et al., 2000). Such modelling can be coupled with laboratory, field, and greenhouse studies regarding plant and bacterial adaptations to heat, light, and other stresses.

6 Conclusions

This study provides a more appropriate method to partition ecosystem CO_2 fluxes between their upward and downward components by accounting for seasonal changes in base respiration and temperature sensitivity and for the effect of even low levels of light in driving photosynthetic uptake. This new approach to a multi-step bulk method allows a discovery of the effect of early-season higher temperature periods in driving higher respiration (rather than reduced or deactivated uptake) with the net effect of creating a mid-day CO_2 source despite high light conditions. These events seem more likely earlier in the growing season when mosses and plants have not yet fully matured enough to take advantage of the warm, sunny conditions. Such "hot moments" of ecosystem CO_2 emissions may change in frequency depending on changes in the region's synoptic weather conditions. An increase in the frequency of hotter weather conditions, following this study and others, should increase ecosystem respiration with an effect of reducing the net uptake of CO_2 by tundra landscapes.

References

Abnizova, A., Siemens, J., Langer, M., and Boike, J.: Small ponds with major impact: The relevance of ponds and lakes in permafrost landscapes to carbon dioxide emissions, Global Biogeochem. Cy., 26, GB2041, doi:10.1029/2011GB004237, 2012.

Bauerle, W. L., Oren, R., Way, D. A., Qian, S. S., Stoy, P. C., Thornton, P. E., Bowden, J. D., Hoffman, F. M., and Reynolds, R. F.: Photoperiodic Regulation of the Seasonal Pattern of Photosynthetic Capacity and the Implications for Carbon Cycling, P. Natl. Acas. Sci. USA, doi:10.1073/pnas.1119131109, 2012.

Belshe, E. F., Schuur, E. A. G., Bolker, B. M., and Bracho, R.: Incorporating spatial heterogeneity created by permafrost thaw into a landscape carbon estimate, J. Geophys. Res., 117, G01026, doi:10.1029/2011JG001836, 2012.

Berry, J. and Björkman, O.: Photosynthetic response and adaptation to temperature in higher plants, Ann. Rev. Plant Physio., 31, 491–543, 1980.

Boike, J., Hinzman, L., Overduin, P., Romanovsky, V., Ippisch, O., and Roth, K.: A comparison of snow melt at three circumpolar sites: Spitsbergen, Siberia, Alaska, in: Proceedings of the 8th International Conference on Permafrost, Zürich, Switzerland, 21–25, available at: http://www.arlis.org/docs/vol1/ICOP/55700698/Pdf/Chapter_015.pdf (last access: 22 June 2012), 2003.

Boike, J., Hagedorn, B., and Roth, K.: Heat and water transfer processes in permafrost-affected Soils: A review of field-and modeling-based studies for the Arctic and Antarctic, in: Proceedings of NICOP, University of Alaska, Fairbanks, USA, 149–154, 2008.

Boike, J., Kattenstroth, B., Abramova, K., Bornemann, N., Chetverova, A., Fedorova, I., Fröb, K., Grigoriev, M., Grüber, M., Kutzbach, L., Langer, M., Minke, M., Muster, S., Piel, K., Pfeiffer, E.-M., Stoof, G., Westermann, S., Wischnewski, K., Wille, C., and Hubberten, H.-W.: Baseline characteristics of climate, permafrost, and land cover from a new permafrost observatory in the Lena River Delta, Siberia (1998–2011), Biogeosciences Discuss., 9, 13627–13684, doi:10.5194/bgd-9-13627-2012, 2012.

Brooks, A. and Farquhar, G. D.: Effect of temperature on the CO_2/O_2 specificity of ribulose-1,5-bisphosphate carboxylase oxygenase and the rate of respiration in the light - estimates from gas-exchange measurements on spinach, Planta, 165, 397–406, 1985.

Deser, C., Walsh, J. E., and Timlin, M. S.: Arctic sea ice variability in the context of recent atmospheric circulation trends, J. Climate, 13, 617–633, 2000.

Falge, E., Baldocchi, D., Olson, R., Anthoni, P., Aubinet, M., Bernhofer, C., Burba, G., Ceulemans, R., Clement, R., Dolman, H., Granier, A., Gross, P., Grunwald, T., Hollinger, D., Jensen, N. O., Katul, G., Keronen, P., Kowalski, A., Lai, C. T., Law, B. E., Meyers, T., Moncrieff, H., Moors, E., Munger, J. W., Pilegaard, K., Rannik, U., Rebmann, C., Suyker, A., Tenhunen, J., Tu, K., Verma, S., Vesala, T., Wilson, K., and Wofsy, S.: Gap filling strategies for defensible annual sums of net ecosystem exchange, Agr. Forest. Meteorol., 107, 43–69, 2001.

Falge, E., Baldocchi, D., Tenhunen, J., Aubinet, M., Bakwin, P., Berbigier, P., Bernhofer, C., Burba, G., Clement, R., Davis, K. J., Elbers, J. A., Goldstein, A. H., Grelle, A., Granier, A., Guomundsson, J., Hollinger, D., Kowalski, A. S., Katul, G., Law, B. E., Malhi, Y., Meyers, T., Monson, R. K., Munger, J. W., Oechel, W., Paw, K. T., Pilegaard, K., Rannik, U., Rebmann, C., Suyker, A., Valentini, R., Wilson, K., and Wofsy, S.: Seasonality of ecosystem respiration and gross primary production as derived from FLUXNET measurements, Agr. Forest. Meteor., 113, 53–74, 2002.

Foken, T. and Wichura, B.: Tools for quality assessment of surface-based flux measurements, Agr. Forest Meteor., 78, 83–105, doi:10.1016/0168-1923(95)02248-1, 1996.

Furness, S. B. and Grime, J. P.: Growth Rate and Temperature Responses in Bryophytes: II. A Comparative Study of Species of Contrasted Ecology, J. Ecol., 70, 525–536, doi:10.2307/2259920, 1982.

Grigoriev, N.: The temperature of permafrost in the Lena delta basin–deposit conditions and properties of the permafrost in Yakutia, Yakutsk, 2, 97–101, 1960.

Groendahl, L., Friborg, T., and Soegaard, H.: Temperature and snow-melt controls on interannual variability in carbon exchange in the high Arctic, Theor. Appl. Climatol., 88, 111–125, doi:10.1007/s00704-005-0228-y, 2007.

Hájek, T., Tuittila, E.-S., Ilomets, M., and Laiho, R.: Light responses of mire mosses – a key to survival after water-level drawdown?, Oikos, 118, 240–250, doi:10.1111/j.1600-0706.2008.16528.x, 2009.

Haxeltine, A. and Prentice, I. C.: A general model for the light-use efficiency of primary production, Funct. Ecol., 10, 551–561, 1996.

Helbig, M., Boike, J., Langer, M., Schreiber, P., Runkle, B. R. K., and Kutzbach, L.: Spatial and seasonal variability of polygonal tundra water balance: Lena River Delta, northern Siberia (Russia), Hydrogeol. J., 21, 133–147, doi:10.1007/s10040-012-0933-4, 2013.

Henley, W. J., Levavasseur, G., Franklin, L. A., Osmond, C. B., and Ramus, J.: Photoacclimation and photoinhibition inUlva rotundata as influenced by nitrogen availability, Planta, 184, 235–243, doi:10.1007/BF01102423, 1991.

Höfle, S., Rethemeyer, J., Mueller, C. W., and John, S.: Organic matter composition and stabilization in a polygonal tundra soil

of the Lena-Delta, Biogeosciences Discuss., 9, 12343–12376, doi:10.5194/bgd-9-12343-2012, 2012.

Hubberten, H. W., Wagner, D., Pfeiffer, E., Boike, J., and Gukov, A. Y.: The Russian-German research station Samoylov, Lena Delta – a key site for polar research in the Siberian arctic, Polarforschung, 73, 111–116, 2006.

Ibrom, A., Dellwik, E., Larsen, S. E., and Pilegaard, K.: On the use of the Webb-Pearman-Leuning theory for closed-path eddy correlation measurements, Tellus B, 59, 937–946, 2007.

Johannessen, O. M., Bengtsson, L., Miles, M. W., Kuzmina, S. I., Semenov, V. A., Alekseev, G. V., Nagurnyi, A. P., Zakharov, V. F., Bobylev, L. P., Pettersson, L. H., Hasselmann, K., and Cattle, H. P.: Arctic climate change: observed and modelled temperature and sea-ice variability, Tellus A, 56, 328–341, doi:10.1111/j.1600-0870.2004.00060.x, 2004.

Kutzbach, L.: The exchange of energy, water and carbon dioxide between wet arctic tundra and the atmosphere at the Lena River Delta, Northern Siberia, Reports on Polar and Marine Research 541, Alfred Wegener Institute, Bremerhaven, Germany, Ph.D. thesis, University of Hamburg, 157 pp., 2006.

Kutzbach, L., Wagner, D., and Pfeiffer, E. M.: Effect of microrelief and vegetation on methane emission from wet polygonal tundra, Lena Delta, Northern Siberia, Biogeochemistry, 69, 341–362, 2004.

Kutzbach, L., Wille, C., and Pfeiffer, E.-M.: The exchange of carbon dioxide between wet arctic tundra and the atmosphere at the Lena River Delta, Northern Siberia, Biogeosciences, 4, 869–890, doi:10.5194/bg-4-869-2007, 2007.

Lasslop, G., Reichstein, M., Papale, D., Richardson, A. D., Arneth, A., Barr, A., Stoy, P., and Wohlfahrt, G.: Separation of net ecosystem exchange into assimilation and respiration using a light response curve approach: critical issues and global evaluation, Glob. Change Biol., 16, 187–208, doi:10.1111/j.1365-2486.2009.02041.x, 2010.

Lasslop, G., Migliavacca, M., Bohrer, G., Reichstein, M., Bahn, M., Ibrom, A., Jacobs, C., Kolari, P., Papale, D., Vesala, T., Wohlfahrt, G., and Cescatti, A.: On the choice of the driving temperature for eddy-covariance carbon dioxide flux partitioning, Biogeosciences, 9, 5243–5259, doi:10.5194/bg-9-5243-2012, 2012.

Leuning, R.: The correct form of the Webb, Pearman and Leuning equation for eddy fluxes of trace gases in steady and non-steady state, horizontally homogeneous flows, Bound.-Lay. Meteorol., 123, 263–267, doi:10.1007/s10546-006-9138-5, 2007.

Long, S. P., Humphries, S., and Falkowski, P. G.: Photoinhibition of Photosynthesis in Nature, Annu. Rev. Plant Phys., 45, 633–662, doi:10.1146/annurev.pp.45.060194.003221, 1994.

Loranty, M. M., Goetz, S. J., Rastetter, E. B., Rocha, A. V., Shaver, G. R., Humphreys, E. R., and Lafleur, P. M.: Scaling an Instantaneous Model of Tundra NEE to the Arctic Landscape, Ecosystems, 14, 76–93, doi:10.1007/s10021-010-9396-4, 2010.

Lund, M., Falk, J. M., Friborg, T., Mbufong, H. N., Sigsgaard, C., Soegaard, H., and Tamstorf, M. P.: Trends in CO_2 exchange in a high Arctic tundra heath, 2000–2010, J. Geophys. Res., 117, G02001, doi:10.1029/2011JG001901, 2012.

Mahecha, M. D., Reichstein, M., Carvalhais, N., Lasslop, G., Lange, H., Seneviratne, S. I., Vargas, R., Ammann, C., Arain, M. A., Cescatti, A., Janssens, I. A., Migliavacca, M., Montagnani, L., and Richardson, A. D.: Global Convergence in the Temperature Sensitivity of Respiration at Ecosystem Level, Science, 329, 838–840, doi:10.1126/science.1189587, 2010.

McGuire, A. D., Anderson, L. G., Christensen, T. R., Dallimore, S., Guo, L., Hayes, D. J., Heimann, M., Lorenson, T. D., Macdonald, R. W., and Roulet, N.: Sensitivity of the carbon cycle in the Arctic to climate change, Ecol. Monogr., 79, 523–555, doi:10.1890/08-2025.1, 2009.

Medlyn, B. E., Dreyer, E., Ellsworth, D., Forstreuter, M., Harley, P. C., Kirschbaum, M. U. F., Le Roux, X., Montpied, P., Strassemeyer, J., Walcroft, A., Wang, K., and Loustau, D.: Temperature response of parameters of a biochemically based model of photosynthesis. II. A review of experimental data, Plant Cell Environ., 25, 1167–1179, 2002.

Moncrieff, J. B., Malhi, Y., and Leuning, R.: The propagation of errors in long-term measurements of land-atmosphere fluxes of carbon and water, Glob. Change Biol., 2, 231–240, doi:10.1111/j.1365-2486.1996.tb00075.x, 1996.

Moore, C. J.: Frequency response corrections for eddy correlation systems, Bound.-Lay. Meteorol., 37, 17–35, 1986.

Murray, K. J., Tenhunen, J. D., and Nowak, R. S.: Photoinhibition as a control on photosynthesis and production of Sphagnum mosses, Oecologia, 96, 200–207, 1993.

Nakai, T., Van Der Molen, M. K., Gash, J. H. C., and Kodama, Y.: Correction of sonic anemometer angle of attack errors, Agr. Forest Meteorol., 136, 19–30, 2006.

Oechel, W. C.: Seasonal patterns of temperature response of CO_2 flux and acclimation in arctic mosses growing in situ, Photosynthetica, 10, 447–456, 1976.

ORNL DAAC: MODIS subsetted land products, Collection 5, Oak Ridge National Laboratory Distributed Active Archive Center, Oak Ridge, Tennessee, USA, available on-line: http://daac.ornl.gov/MODIS/modis.html, 2013.

Parmentier, F. J. W., Molen, M. K. van der, Huissteden, J. van, Karsanaev, S. A., Kononov, A. V., Suzdalov, D. A., Maximov, T. C., and Dolman, A. J.: Longer growing seasons do not increase net carbon uptake in the northeastern Siberian tundra, J. Geophys. Res., 116, G04013, doi:10.1029/2011JG001653, 2011.

Pop, E. W., Oberbauer, S. F., and Starr, G.: Predicting Vegetative Bud Break in Two Arctic Deciduous Shrub Species, Salix pulchra and Betula nana, Oecologia, 124, 176–184, doi:10.1007/s004420050005, 2000.

Rastetter, E., Williams, M., Griffin, K., Kwiatkowski, B., Tomasky, G., Potosnak, M., Stoy, P., Shaver, G., Stieglitz, M., Hobbie, J. and Kling, G.: Processing Arctic Eddy-Flux Data Using a Simple Carbon-Exchange Model Embedded in the Ensemble Kalman Filter, Ecol. Appl., 20, 1285–1301, doi:10.1890/09-0876.1, 2009.

Reichstein, M., Falge, E., Baldocchi, D., Papale, D., Aubinet, M., Berbigier, P., Bernhofer, C., Buchmann, N., Gilmanov, T., Granier, A., Grunwald, T., Havrankova, K., Ilvesniemi, H., Janous, D., Knohl, A., Laurila, T., Lohila, A., Loustau, D., Matteucci, G., Meyers, T., Miglietta, F., Ourcival, J.-M., Pumpanen, J., Rambal, S., Rotenberg, E., Sanz, M., Tenhunen, J., Seufert, G., Vaccari, F., Vesala, T., Yakir, D., and Valentini, R.: On the separation of net ecosystem exchange into assimilation and ecosystem respiration: review and improved algorithm, Glob. Change Biol., 11, 1424–1439, doi:10.1111/j.1365-2486.2005.001002.x, 2005.

Riutta, T., Laine, J., and Tuittila, E.-S.: Sensitivity of CO_2 Exchange of Fen Ecosystem Components to Water Level Variation,

Ecosystems, 10, 718–733, 2007.

Sachs, T., Giebels, M., Boike, J., and Kutzbach, L.: Environmental controls on CH4 emission from polygonal tundra on the microsite scale in the Lena river delta, Siberia, Glob. Change Biol., 16, 3096–3110, doi:10.1111/j.1365-2486.2010.02232.x, 2010.

Sachs, T., Wille, C., Boike, J., and Kutzbach, L.: Environmental controls on ecosystem-scale CH4 emission from polygonal tundra in the Lena River Delta, Siberia, J. Geophys. Res,, 113, G00A03, doi:10.1029/2007JG000505, 2008.

Schotanus, P., Nieuwstadt, F. T. M., and Bruin, H. A. R.: Temperature measurement with a sonic anemometer and its application to heat and moisture fluxes, Bound.-Lay. Meteorol, 26, 81–93, 1983.

Serreze, M. C. and Barry, R. G.: Processes and impacts of Arctic amplification: A research synthesis, Global Planet, Change, 77, 85–96, doi:10.1016/j.gloplacha.2011.03.004, 2011.

Serreze, M. and Francis, J.: The Arctic Amplification Debate, Climatic Change, 76, 241–264, doi:10.1007/s10584-005-9017-y, 2006.

Shaver, G. R., Street, L. E., Rastetter, E. B., Van Wijk, M. T., and Williams, M.: Functional convergence in regulation of net CO_2 flux in heterogeneous tundra landscapes in Alaska and Sweden, Ecology, 95, 802–817, 2007.

Sveinbjörnsson, B. and Oechel, W. C.: The Effect of Temperature Preconditioning on the Temperature Sensitivity of Net CO_2 Flux in Geographically Diverse Populations of the Moss Polytrichum Commune, Ecology, 64, 1100–1108, doi:10.2307/1937820, 1983.

Thormann, M. N., Bayley, S. E., and Currah, R. S.: Microcosm tests of the effects of temperature and microbial species number on the decomposition of Carex aquatilis and Sphagnum fuscum litter from southern boreal peatlands, Can. J. Microbiol., 50, 793–802, 2004.

Tissue, D. T. and Oechel, W. C.: Response of Eriophorum Vaginatum to Elevated CO_2 and Temperature in the Alaskan Tussock Tundra, Ecology, 68, 401–410, doi:10.2307/1939271, 1987.

van't Hoff, J. H.: Lectures on Theoretical and Physical Chemistry, Part 1: Chemical Dynamics, Edward Arnold, London, 1898.

Vickers, D. and Mahrt, L.: Quality Control and Flux Sampling Problems for Tower and Aircraft Data, J. Atmos. Ocean. Tech., 14, 512–526, doi:10.1175/1520-0426(1997)014¡0512:QCAFSP¿2.0.CO;2, 1997.

Webb, E. K., Pearman, G. I., and Leuning, R.: Correction of flux measurements for density effects due to heat and water vapour transfer, Q. J. Roy. Meteor. Soc., 106, 85–100, 1980.

Wesely, M. L. and Hart, R. L.: Variability of Short Term Eddy-Correlation Estimates of Mass Exchange, in: The Forest-Atmosphere Interaction Proceedings of the Forest Environmental Measurements Conference held at Oak Ridge, Tennessee, 23–28 October 1983, edited by: Hutchison, B. A. and Hicks, B. B., 591–612, 1985.

Wille, C., Kutzbach, L., Sachs, T., Wagner, D., and Pfeiffer, E.-M.: Methane emission from Siberian arctic polygonal tundra: eddy covariance measurements and modeling, Glob. Change Biol, 14, 1395–1408, doi:10.1111/j.1365-2486.2008.01586.x, 2008.

Williams, M. and Rastetter, E. B.: Vegetation characteristics and primary productivity along an arctic transect: implications for scaling-up, J. Ecol., 87, 885–898, doi:10.1046/j.1365-2745.1999.00404.x, 1999.

Williams, T. G. and Flanagan, L. B.: Measuring and modelling environmental influences on photosynthetic gas exchange in Sphagnum and Pleurozium, Plant Cell Environ., 21, 555–564, 1998.

Wohlfahrt, G., Anfang, C., Bahn, M., Haslwanter, A., Newesely, C., Schmitt, M., Drösler, M., Pfadenhauer, J., and Cernusca, A.: Quantifying nighttime ecosystem respiration of a meadow using eddy covariance, chambers and modelling, Agr. Forest Meteorol., 128, 141–162, 2005.

Yvon-Durocher, G., Caffrey, J. M., Cescatti, A., Dossena, M., Del Giorgio, P., Gasol, J. M., Montoya, J. M., Pumpanen, J., Staehr, P. A., Trimmer, M., Woodward, G., and Allen, A. P.: Reconciling the temperature dependence of respiration across timescales and ecosystem types, Nature, 487, 472–476, doi:10.1038/nature11205, 2012.

Zamolodchikov, D. G., Karelin, D. V., Ivaschenko, A. I., Oechel, W. C., and Hastings, S. J.: CO_2 flux measurements in Russian Far East tundra using eddy covariance and closed chamber techniques, Tellus B, 55, 879–892, doi:10.1046/j.1435-6935.2003.00074.x, 2003.

Zona, D., Oechel, W. C., Richards, J. H., Hastings, S., Kopetz, I., Ikawa, H., and Oberbauer, S.: Light-stress avoidance mechanisms in a *Sphagnum*-dominated wet coastal Arctic tundra ecosystem in Alaska, Ecology, 92, 633–644, doi:10.1890/10-0822.1, 2011.

Zubrzycki, S., Kutzbach, L., Grosse, G., Desyatkin, A., and Pfeiffer, E.-M.: Organic carbon and total nitrogen stocks in soils of the Lena River Delta, Biogeosciences Discuss., 9, 17263–17311, doi:10.5194/bgd-9-17263-2012, 2012.